Available online at www.sciencedirect.com

SCIENCE DIRECT®

Inorganica Chimica Acta 357 (2004) 1538–1548

Inorganica Chimica Acta

www.elsevier.com/locate/ica

The mononuclear and dinuclear dimethoxyethane adducts of lanthanide trichlorides $[LnCl_3(DME)_2]_n$, $n = 1$ or 2, fundamental starting materials in lanthanide chemistry: preparation and structures

Ulrich Baisch [1], Daniela Belli Dell'Amico, Fausto Calderazzo, Roberto Conti, Luca Labella, Fabio Marchetti *, Elsje Alessandra Quadrelli [2]

Dipartimento di Chimica e Chimica Industriale, Università di Pisa, via del Risorgimento 35, I-56126 Pisa, Italy

Received 4 November 2003; accepted 8 November 2003

Abstract

Some new dimethoxyethane (DME) adducts of lanthanide trichlorides of formula $[LnCl_3(DME)_2]_n$, $n = 1$ or 2; ($n = 2$, Ln = La, Ce, Pr, Nd; $n = 1$, Ln = Eu, Tb, Ho, Tm, Lu) have been prepared by treating Ln_2O_3, or $LnCl_3 \cdot nH_2O$, or $Ln_2(CO_3)_3$, in DME as medium, with thionyl chloride at room temperature, eventually in the presence of water in the case of Ln_2O_3 and $Ln_2(CO_3)_3$. The complexes from lanthanum to praseodymium included are chloro-bridged dimers. In the case of neodymium, the new results complement the literature data, showing that both the mononuclear and dinuclear species exist: neodymium can therefore be regarded as the turning element from dinuclear to mononuclear structures along the series. Only mononuclear complexes were isolated in the Eu–Lu sequence. The lanthanide contraction has been evaluated on the basis of the Ln–O and Ln–Cl bond distances on the isotypical series of the mononuclear complexes $LnCl_3(DME)_2$ covering a range of 12 atomic numbers.

Keywords: Lanthanide complexes; Chloride complexes

1. Introduction

Lanthanides continue to attract interest in both scientific and technological fields, leading to traditional and new applications. Thus, the industrial applications to ceramic enamels, magnetic materials, and optical glasses have recently been extended, for instance, to Er-doped optical fibers [1] or to lanthanide-based catalysis for diolefin polymerization [2]. Lanthanides are also used in luminescence [3], in NMR spectrometry and in organic synthesis [4]. When operating in non-aqueous systems, the anhydrous trichlorides $LnCl_3$ are the most frequently used starting materials for the preparation of many useful derivatives. Our method for preparing the anhydrous trichlorides was reported in an earlier preliminary communication [5] to give substantially quantitative yields of the dimethoxyethane (DME) adducts of neodymium, europium, and gadolinium. It consists of treating the readily available oxide with the three-component system $SOCl_2/DME/H_2O$ at room temperature, whereby the addition of the appropriate, in principle catalytic, amount of water generates HCl in situ, which is used to convert the oxide, a primary product of the lanthanide technology, into the chloride. The higher coordinating power of DME with respect to $SOCl_2$ excludes the formation of the adducts with thionyl chloride. Later methods using the metal oxide as starting material employ HCl generated in situ from chlorotri-

---

* Corresponding author. Tel.: +390502919233; fax: +390502919246. *E-mail address:* Fama@dcci.unipi.it (F. Marchetti).

[1] Present address: Department Chemie der Ludwig-Maximilians-Universität München, Butenandtstrasse 5-13 (Haus D), D-81377 München, Germany.

[2] Present address: Laboratoire de Chimie Organométallique de Surface UMR9986 – CNRS CPE, Boulevard du 11 Novembre 1918, 43, BP 2077, F-69616 Villeurbanne, France.

0020-1693/$ - see front matter © 2003 Elsevier B.V. All rights reserved.
doi:10.1016/j.ica.2003.11.011

methylsilane and water [6]. Otherwise, the appropriate bulk metal is sonicated with hexachloroethane in the ether as medium [7]. The new preparative methods (vide infra) [5–7] to anhydrous lanthanide chlorides appear to be more facile than those based on the traditional high-temperature (200 °C or higher) reaction of the lanthanide oxide with ammonium chloride [8a], or on the treatment of the lanthanide metal with a chlorinating agent ($HgCl_2$) [8b].

The present paper, beside extending the $SOCl_2$/DME/H_2O methodology [5] to La_2O_3, thus covering a range of 8 atomic numbers along the lanthanide series (from lanthanum to gadolinium included), reports that anhydrous lanthanide chlorides can also be prepared from the carbonate [the example of $Er_2(CO_3)_3(H_2O)_2$ is explicitly presented in Section 2 or from the hydrated chloride, simply by treating the starting material with thionyl chloride at room temperature. As the hydrated chlorides can be easily obtained from the oxide and aqueous hydrochloric acid, this paper discloses three different methods of preparing the DME adducts of the anhydrous lanthanide chlorides, all operating at room temperature and with easily available reagents.

At the onset of this work, lanthanide trichlorides in the presence of an oxygen donor were known to form ionic or low-nuclearity species, for instance $Ln_2Cl_6(THF)_7$, i.e. $[LnCl_2(THF)_5]^+[LnCl_4(THF)_2]^-$, or $LnCl_3(DME)_2$, $LnCl_3(THF)_4$, or the chloride-bridged dimer $Yb_2Cl_6(THF)_4$ [9]. In our preliminary communication [5] we had already noted that the europium(III) derivative of formula $EuCl_3(DME)_2$ is isostructural with both the gadolinium [10] and yttrium analogs [11]. At the present time, structural characterization of some mononuclear $LnCl_3(DME)_2$ species has been achieved (Ln = Nd [12], Dy [9a], Er [7b,9b], Yb [7b]) showing these compounds to be isotypical with each other and with the yttrium derivative $YCl_3(DME)_2$ [11].

Moreover, structural data have recently been reported by an Australian group on the dinuclear trichloro-dimethoxyethane derivative of neodymium of formula $Nd_2Cl_6(DME)_4$. The Authors have noted that this chloride-bridged dimer contains octacoordinated neodymium and they have indicated that "*it remains to be determined where the transition point from eight coordinate to seven coordinate occurs and the structure of SmCl₃(dme)₂ is needed to resolve this.*" [9c]. As it was somewhat intriguing that neodymium could give both the mononuclear [12] and the dinuclear derivatives, it was in order to clarify and rationalize several structural aspects of this important class of lanthanide derivatives.

The present paper reports new crystal data on the mononuclear species in the sequence from europium to lutetium, see Table 1. Furthermore, it still remained to be established which are the typical crystal structures for the elements from lanthanum to praseodymium, i.e. in the early part of the lanthanide sequence. Our paper reports the X-ray structures of the *dinuclear* lanthanum(III), cerium(III) and praseodymium(III) derivatives, see Table 2. Thus, neodymium, for which both the mononuclear and the dinuclear structures are known, appears to be the turning point from dinuclear (CN eight for the lanthanide) to mononuclear (CN seven for the central metal atom) structures.

A further point of interest is represented by the observation that for isostructural series of compounds, the experimentally observed interatomic parameters can be utilized for an evaluation of the ionic radii along the lanthanide series [13]. It is to be pointed out that the so-called lanthanide contraction is based on crystal data collected around the fifties of the past

Table 1
Crystal data and structure refinement of the isotypical, monoclinic, space group $P2_1/c$, lanthanide complexes $LnCl_3(DME)_2$

Lanthanide	Eu	Tb	Ho	Tm	Lu
Empirical formula	$C_8H_{20}Cl_3EuO_4$	$C_8H_{20}Cl_3O_4Tb$	$C_8H_{20}Cl_3HoO_4$	$C_8H_{20}Cl_3O_4Tm$	$C_8H_{20}Cl_3LuO_4$
Formula weight	438.55	445.51	451.52	455.52	461.56
Temperature (K)	208(2)	293(2)	293(2)	293(2)	293(2)
a (Å)	11.506(1)	11.501(2)	11.456(1)	11.4166(9)	11.371(2)
b (Å)	8.9044(7)	8.941(1)	8.9272(8)	8.9161(7)	8.889(2)
c (Å)	15.644(2)	15.670(2)	15.660(1)	15.633(1)	15.606(4)
β (°)	104.92(1)	105.02(1)	104.962(7)	104.919(7)	104.825(15)
Volume (Å^3)	1548.8(3)	1556.2(4)	1547.3(2)	1537.7(2)	1524.9(6)
Z	4	4	4	4	4
ρ_{calc} (Mg/m^3)	1.881	1.902	1.938	1.968	2.010
μ (mm^{-1})	4.563	5.056	5.628	6.287	6.995
Data/restraints/parameters	3715/0/145	2746/0/146	3785/0/150	3007/0/145	2692/0/146
$R(F_o)[I > 2\sigma(I)]$[a]	0.0311	0.0323	0.0350	0.0475	0.0543
$R_w(F_o^2)[I > 2\sigma(I)]$[a]	0.0708	0.0788	0.0939	0.1061	0.1351
Goodness-of-fit on F^2[a]	1.019	1.039	0.830	1.019	1.012

[a] $R(F_o) = \sum ||F_o| - |F_c|| / \sum |F_o|$; $R_w(F_o^2) = \left[\sum[w(F_o^2 - F_c^2)^2] \Big/ \sum[wF_o^2)^2] \right]^{1/2}$; $w = 1/[\sigma^2(F_o^2) + (AQ)^2 + BQ]$, where $Q = [\max(F_o^2, 0) + 2F_c^2]/3$; Goodness-of-fit $= \left[\sum[w(F_o^2 - F_c^2)^2]/(N - P) \right]^{1/2}$, where N and P are the numbers of observations and parameters, respectively.

Table 2
Crystal data at 293 K and structure refinement of $Ln_2Cl_6(DME)_4$ complexes

Lanthanide	La[a]	Ce[a]	Pr[a]	Nd[a]	Nd[b]	Pr[c]
Empirical formula	$C_{16}H_{40}Cl_6La_2O_8$	$C_{16}H_{40}Cl_6Ce_2O_8$	$C_{16}H_{40}Cl_6O_8Pr_2$	$C_{16}H_{40}Cl_6Nd_2O_8$	$C_{20}H_{50}Cl_6Nd_2O_{10}$	$C_{16}H_{40}Cl_6O_8Pr_2$
Formula weight	851.00	853.42	855.00	861.66	951.78	855.00
Space group	$P2_1/n$	$P2_1/n$	$P2_1/n$	$P2_1/n$	$P\bar{1}$	$P2_1/n$
a (Å)	10.947(3)	10.929(1)	10.907(2)	10.898(1)	8.645(2)	8.474(3)
b (Å)	12.992(3)	12.983(1)	12.956(2)	12.935(1)	9.322(1)	18.149(5)
c (Å)	11.225(7)	11.200(1)	11.163(1)	11.132(1)	12.676(2)	10.569(2)
α (°)					88.597(6)	
β (°)	102.51(5)	102.31(1)	102.24(2)	102.16(1)	83.88(1)	109.16(3)
γ (°)					65.78(1)	
Volume (Å^3)	1558.6(11)	1552.6(2)	1541.6(4)	1534.0(2)	926.1(3)	1535.4(7)
Z	2	2	2	2	1	2
ρ_{calc} (Mg/m^3)	1.813	1.825	1.842	1.865	1.707	1.849
μ (mm^{-1})	3.251	3.444	3.676	3.903	3.245	3.691
Data/restraints/parameters	2437/0/149	2607/0/149	2590/0/149	2303/0/149	2520/0/177	2533/0/149
$R(F_o)[I > 2\sigma(I)]$[d]	0.0579	0.0289	0.0239	0.0308	0.0287	0.0224
$R_w(F_o^2)[I > 2\sigma(I)]$[d]	0.1391	0.0670	0.0674	0.0691	0.0728	0.0594
Goodness-of-fit on F^2[d]	2.097	0.998	1.207	1.005	1.084	1.154

[a] α-Phase.
[b] $Nd_2Cl_6(DME)_4 \cdot DME$.
[c] β-Phase.
[d] See Table 1.

century on the fluorides and oxides [14], which are not isostructural all along the series. Thus, the observed trend of the Ln–ligand distance vs. the f^n electronic configuration of the lanthanide ion for *isostructural* series of molecular compounds is of special significance. This is done, in our paper, for both the Ln–O and the Ln–Cl bond distances, i.e. for five different sets of data.

2. Experimental

Solvents were freshly distilled over the conventional drying agents under a controlled atmosphere (dinitrogen or argon). The reactions were carried out under an initial atmosphere of dinitrogen or argon. In this connection, it is important to realize that since gases (HCl, SO_2, CO_2) are produced during the preparation of the anhydrous lanthanide chlorides, the initial anhydrous conditions can be maintained simply by using a no-return valve filled with an inert liquid (usually Nujol) in order to keep the content of the reaction flask separated from the external atmosphere. Some of the lanthanide oxides (Nd_2O_3, Sm_2O_3, Gd_2O_3) were supplied by Rhône-Poulenc. Commercial (Aldrich, C. Erba, Fluka, Strem) hydrated cerium, praseodymium, erbium and lutetium trichlorides were used. The hydrated trichlorides of terbium, holmium, thulium and ytterbium were prepared by heating the metal oxide (Ln_2O_3, with the exception of terbium for which Tb_4O_7 [15a] was used) with concentrated aqueous HCl. The resulting solution was then evaporated to dryness in vacuo at ca. 50 °C. Residues analysing as $TbCl_3(H_2O)_5$ (colourless), $HoCl_3(H_2O)_{5.5}$ (yellow), $TmCl_3(H_2O)_6$ (colourless), $YbCl_3(H_2O)_6$ (colourless) were obtained in substantially quantitative yields. Elemental analyses were performed for chlorine by the Volhard method and for the lanthanide content by calcining the samples at 850 °C, after treatment with some drops of concentrated HNO_3, and finally by weighing the residue as Ln_2O_3, or as CeO_2, Pr_6O_{11}, Tb_4O_7 [15a]. The IR spectra were measured with a FT-IR Perkin–Elmer mod.1725X spectrophotometer.

2.1. Synthesis of the DME adducts $LnCl_3$ (Ln = La, Nd) from Ln_2O_3

The preparations of the europium and gadolinium complexes $LnCl_3(DME)_2$, Ln = Eu, Gd, from the corresponding oxides were reported in our preliminary communication [5] and will not be repeated here. The preparation of the neodymium derivative, already announced earlier [5], is reported here for some important details concerning the crystallization of the DME adduct. *Lanthanum.* The oxide La_2O_3 (5.00 g, 15.3 mmol) was suspended in DME (200 cm^3) and thionyl chloride was added (50 cm^3, $d = 1.631$ g × cm^{-3}, 685 mmol). Water (8 cm^3, 444 mmol) was then added at room temperature in about 2.5 h. After 3 days stirring the suspension was filtered under dinitrogen and the colourless solid was dried in vacuo (10^{-2} Torr, ca. 4 h). The product, analysing as $LaCl_3(DME)$, was sealed in vials under dinitrogen (9.67 g, 94% yield). *Anal.* Calc. for $C_4H_{10}Cl_3LaO_2$: Cl, 31.7; La, 41.4. Found: Cl, 31.9; La, 41.4%. IR (1250–850 cm^{-1}, Nujol mull, cm^{-1}): 1234m, 1186m, 1144w, 1082s, 1039s, 1001m, 857s. From the filtrate, stored at 0 °C, colourless crystals separated out, which were chosen, before being dried, for the X-ray diffractometric studies and found to contain the dinuclear molecules $[LaCl_3(DME)_2]_2$ (vide infra). *Neodymium.* The oxide Nd_2O_3 (4.56 g, 13.5 mmol) was suspended in DME (100 cm^3) and thionyl chloride (30 cm^3, 411 mmol) and water (4 cm^3, 222 mmol) were added at room temperature over about 2 h. After 1 day stirring, the suspension was filtered under dinitrogen and the violet solid was dried in vacuo (10^{-2} Torr, ca. 6 h). The product was collected under dinitrogen and shown to have the analytical composition $NdCl_3(DME)$ (7.99 g, 87% yield). *Anal.* Calc. for $C_4H_{10}Cl_3NdO_2$: Cl, 31.2; Nd, 42.3. Found: Cl, 32.3; Nd, 43.2%. IR (1250–850 cm^{-1}, Nujol mull, cm^{-1}): 1243m, 1162w, 1117s, 1049s, 1027s, 863s. Violet crystals of $Nd_2Cl_6(DME)_4$ separated out from the filtrate at 0 °C: they were isolated by filtration and used for the X-ray diffractometric studies.

The samarium derivative was also obtained by a similar procedure starting from Sm_2O_3. The pale yellow DME adduct of $SmCl_3$, analysing correctly as $SmCl_3(DME)_2$, was also synthesized and used as an intermediate to the corresponding *N,N*-di-*iso*-propylcarbamato derivative [15b].

The oxides of terbium and ytterbium, Tb_4O_7 and Yb_2O_3 were unaffected by the treatment with $SOCl_2/H_2O/DME$, the metal oxide being recovered unchanged.

2.2. Synthesis of the DME adducts of $LnCl_3$ (Ln = Ce, Pr, Tb, Ho, Er, Tm, Yb, Lu) from the hydrated chloride

The syntheses were carried out in DME starting from $LnCl_3(H_2O)_x$ by using $SOCl_2$ as dehydrating agent. *Cerium.* The commercial product $CeCl_3(H_2O)_7$ (9.78 g, 24.9 mmol) was suspended in DME (100 cm^3) and thionyl chloride was added (25 cm^3, 343 mmol) from a dropping funnel in 2 h. After 1 day stirring the suspension was filtered under dinitrogen and the colourless solid was dried in vacuo (10^{-2} Torr, ca. 5 h). The resulting product, analysing as $CeCl_3(DME)$, was sealed in vials under dinitrogen (8.29 g, 99% yield). *Anal.* Calc. for $C_4H_{10}CeCl_3O_2$: Cl, 31.6; Ce, 41.6. Found: Cl, 31.3; Ce, 41.8%. IR (1250–850 cm^{-1}, Nujol mull, cm^{-1}): 1233m, 1107m, 1082s, 1039s, 859s. The product was recrystallized from DME: at 0 °C colourless crystals of $Ce_2Cl_6(DME)_4$ separated out and were used for the X-ray diffractometric experiment, see Table 2. *Praseodymium.* By using the same procedure described for cerium, starting from $PrCl_3(H_2O)_6$, the light yellow–green product, analyzing as $PrCl_3(DME)$, was obtained (78% yield). *Anal.* Calc. for $C_4H_{10}Cl_3O_2Pr$: Cl, 31.5; Pr, 41.8. Found: Cl, 31.9; Pr, 41.6%. IR (1250–850 cm^{-1}, Nujol mull, cm^{-1}): 1250w, 1234m, 1185w, 1144w, 1108m, 1082s, 1039s, 997w, 859s. The filtrate, stored at about 0 °C, separated out pale yellow crystals of $Pr_2Cl_6(DME)_4$.

2.3. The $LnCl_3(DME)_2$ derivatives

By using the same procedure described for cerium, products analysing as $LnCl_3(DME)_2$ were obtained. *Terbium.* 82% yield. *Anal.* Calc. for $C_8H_{20}Cl_3O_4Tb$: Cl, 23.9; Tb, 35.7. Found: Cl, 23.5; Tb, 36.4%. IR (1250–850 cm^{-1}, Nujol mull, cm^{-1}): 1250m, 1241m, 1209w, 1153w, 1096vs, 1077s, 1030s, 977w, 859s. Colourless crystals of $TbCl_3(DME)_2$ were obtained from the filtrate at −30 °C. *Holmium.* 80% yield. *Anal.* Calc. for $C_8H_{20}Cl_3HoO_4$: Cl, 23.6; Ho, 36.5. Found: Cl, 23.5; Ho, 37.1%. IR (1250–850 cm^{-1}, Nujol mull, cm^{-1}): 1250m, 1241m, 1209w, 1154w, 1095vs, 1076s, 1031s, 976s, 857s. Pale yellow crystals of $HoCl_3(DME)_2$ were obtained from the filtrate at −30 °C. *Erbium:* 90% yield. *Anal.* Calc. for $C_8H_{20}Cl_3ErO_4$: Cl, 23.4; Er, 36.9. Found: Cl, 22.4; Er, 37.2%. *Thulium.* 85% yield. *Anal.* Calc. for $C_8H_{20}Cl_3O_4Tm$: Cl, 23.4; Tm, 37.1. Found: Cl, 23.1; Tm, 37.6%. IR (1250–850 cm^{-1}, Nujol mull, cm^{-1}): 1250m, 1241m, 1209w, 1153w, 1094m, 1076s, 1032s, 976s, 856s. Colourless crystals of $TmCl_3(DME)_2$ were obtained from the filtrate at about 0 °C. *Ytterbium:* 87% yield. *Anal.* Calc. for $C_8H_{20}Cl_3O_4Yb$: Cl, 23.1; Yb, 37.6. Found: Cl, 22.8; Yb, 37.2%. IR (1250–850 cm^{-1}, KBr pellets, cm^{-1}): 1249m, 1242m, 1209m, 1186m, 1153w, 1117m, 1091s, 1077s, 1032vs, 977m, 861s. Colourless crystals of $YbCl_3(DME)_2$ were obtained from the filtrate at about 0 °C. *Lutetium.* 90% yield. *Anal.* Calc. for $C_8H_{20}Cl_3LuO_4$: Cl, 23.0; Lu, 37.9. Found: Cl, 22.6; Lu, 38.1%. IR (1250–850 cm^{-1}, Nujol mull, cm^{-1}): 1240w, 1185w, 1119m, 1076m, 1029s, 978w. Colourless crystals of $LuCl_3(DME)_2$ were obtained from the filtrate at about 0 °C.

2.4. Synthesis of $ErCl_3(DME)_2$ from $Er_2(CO_3)_3$

The carbonate $Er_2(CO_3)_3(H_2O)_2$ (5.56 g, 20.2 mmol of Er) was suspended in DME (100 cm^3) and thionyl chloride was added (40 cm^3, 548 mmol). Water (4 cm^3, 222 mmol) was then added at room temperature in about 0.5 h, and, after 3 d stirring, the suspension was filtered under argon and the pink solid was dried in vacuo at room temperature (10^{-2} Torr, ca. 6 h). The product analysed as $ErCl_3(DME)_2$ (7.40 g, 81% yield). *Anal.* Calc. for $C_8H_{20}Cl_3ErO_4$: Cl, 23.4; La, 36.9. Found: Cl, 22.7; Er, 37.4%. IR (1250–850 cm^{-1}, KBr pellets, cm^{-1}): 1241m, 1209m, 1186m, 1090s, 1076s, 1032vs, 976m, 858s. The filtrate, stored at 0 °C, separated out pink crystals of the product. Similar results were obtained starting from neodymium carbonate.

2.5. Reaction of Nd_2O_3 with HCl in DME: formation of $NdCl_3(H_2O)(DME)$

Under a N_2 atmosphere, the oxide Nd_2O_3 (29 mmol of Nd) was suspended in DME (100 cm^3) in a 500 cm^3 flask. The flask was then evacuated and connected to an apparatus producing HCl from $NH_4Cl_{(s)}$ and concentrated H_2SO_4. The suspension was stirred till gas absorption had ceased (17 h). The product was recovered by filtration and dried in vacuo at room temperature for 7 h. (10.02 g, 96% yield). *Anal.* Calc. for $NdCl_3(H_2O)(DME)$, $C_4H_{12}Cl_3NdO_3$: Cl, 29.6; Nd, 40.2. Found: Cl, 29.3; Nd, 40.2%. IR (PCTFE and Nujol, cm^{-1}): 3297s, 3168m, 2964w, 2945w,1636w, 1606m, 1559w, 1541w, 1508w, 1304w, 1279m, 1240w, 1192w, 1157w, 1107m, 1097m, 1048s, 1018m, 1011m, 864s, 829w.

2.6. Treatment of $EuCl_3(H_2O)_2$ with DME

The chloride $EuCl_3(H_2O)_2$ (1.79 g, 6.08 mmol) was introduced in a flask containing 100 cm^3 of DME. The suspension was stirred for 21 h at room temperature and the colourless product was recovered by filtration and dried in vacuo at room temperature for 5 h (2.04 g, 87.3% yield). *Anal.* Calc. for $EuCl_3(H_2O)_2(DME)$, C_4H_{14} Cl_3EuO_4: Cl, 27.7; Eu, 39.5. Found: Cl, 27.8; Eu, 38.6%. IR (Nujol, cm^{-1}) 3339s, 1633m, 1606m, 1261w, 1250w, 1241w, 1188w, 1154w, 1104w, 1088w, 1078m, 1037s, 976w, 867s, 830w, 801w. A portion of the product (1.81 g, 4.71 mmol) was further heated with DME at the reflux temperature for 6 h. The solid, collected by filtration, was dried in vacuo for 6 h at room temperature (1.30 g, 75.4% yield). *Anal.* Calc. for $EuCl_3(H_2O)$ (DME), $C_4H_{12}Cl_3$ EuO_3: Cl, 29.0; Eu, 41.5. Found: Cl, 29.1; Eu, 42.8%.

2.7. X-ray crystallography

Only the structure determination of $TbCl_3(DME)_2$ is described, the other determinations being performed in a similar way, see Tables 1 and 2.

The diffractometric measurements were carried out by using a Bruker P4 diffractometer equipped with graphite-monochromated MoKα radiation ($\lambda = 0.71073$ Å). One of the colourless crystals was sealed in a glass capillary under a dinitrogen atmosphere and the unit cell parameters listed in Table 1 were derived from the setting angles of 31 strong reflections. Data were collected in the $\omega/2\theta$ scan mode, and three standard reflections were monitored every 97 measurements for checking crystal decay and equipment stability. Data reduction was carried out by the XSCANS programme [16]. A set of 3621 intensity data were collected between $\theta = 2.6°$ and 25.0° and corrected for Lorentz and polarization effects and for absorption by the ψ-scan method. After merging the equivalent reflections $\{R_{\text{int}} = [\sum |F_o^2 - F_o^2(\text{mean})| / \sum(F_o^2)] = 0.0315\}$, 2746 unique reflections were retained for the following calculations. The systematic absences indicated the $P2_1/c$ space group. The solution was found by direct methods and the molecule was completed in the subsequent difference Fourier maps.

The calculations were done by using the SHELX-97 and SHELXTL programmes [17,18]. In the final refinement cycles based on F^2, anisotropic thermal parameters were used for all non-hydrogen atoms. The final reliability factors are listed in Tables 1 and 2.

3. Results and discussion

As partly announced in a preliminary communication, the oxides Ln_2O_3 of some early lanthanides (Ln = La, Nd, [5] Sm, Eu, [5] Gd [5]) are converted to the corresponding chlorides $[LnCl_3(DME)_2]_n$ by treatment with DME and thionyl chloride at room temperature. The reaction can be represented as shown in the general Eq. (1), which is the sum of the partial Eqs. (1a)–(1c).

$$3H_2O + 3SOCl_2 \rightarrow 3SO_2 + 6HCl \tag{1a}$$

$$Ln_2O_3 + 6HCl \rightarrow 3H_2O + 2LnCl_3 \tag{1b}$$

$$2LnCl_3 + 2n\text{DME} \rightarrow 2LnCl_3(\text{DME})_n \tag{1c}$$

$$\begin{aligned} &Ln_2O_3 + 3SOCl_2 + 2n\text{DME} \\ &\quad \rightarrow 2LnCl_3(\text{DME})_n + 3SO_2. \end{aligned} \tag{1}$$

No reaction occurred between Ln_2O_3 and $SOCl_2$ under similar conditions in the absence of DME/H_2O, in agreement with the observation that chlorination of lanthanide oxides by thionyl chloride requires high temperatures [19]. The reaction must of course be carried out in the presence of a defective amount of water with respect to $SOCl_2$, and the attack of the metal oxide is believed to be carried out by the hydrogen chloride produced in situ, see reaction (1a). Although a catalytic amount of water is in principle required, reasonable reaction rates are obtained if enough water is present to nominally produce a two-molar excess of HCl with respect to the stoichiometry of Eq. (1b). A twofold molar excess of thionyl chloride with respect to water is employed in order to maintain the system under final anhydrous conditions. In this connection, it is remarkable that the presence of thionyl chloride is essential for the formation of the anhydrous etherate of $LnCl_3$: as a matter of fact, in the case of neodymium, it has been shown that the oxide Nd_2O_3, treated with dry HCl in DME produces the aquo complex of analytical composition $NdCl_3(H_2O)$ (DME). Similar general behavior is expected for other lanthanide oxides.

It is to be noted that due to the higher coordinating power of DME with respect to thionyl chloride [20], no case was ever observed of $SOCl_2$ being coordinated to the final product. The rather strong coordinating power of DME is also considered to be an important factor in the successful formation of the anhydrous chlorides, since coordination by DME presumably leads to more soluble species of lower nuclearity. It has in fact been found that addition of DME to $EuCl_3(H_2O)_2$ produces the DME adduct $EuCl_3(H_2O)_2(DME)$, or $EuCl_3(H_2O)(DME)$, depending on temperature. Finally, it is to be observed that although in principle this methodology operates also with tetrahydrofuran (THF) as reported earlier [5], the use of DME is preferred because THF may dehydrate, as some of us have observed under certain conditions [21].

The $SOCl_2/H_2O/DME$ reaction works well for the synthesis of the $LnCl_3(DME)_n$ adducts of the lighter lanthanides. For the heavier elements, we have found it more convenient to prepare the Tb, Ho, Er, Tm, Yb and Lu compounds by dehydrating the easily accessible lanthanide chlorides with $SOCl_2$ in DME, see Eq. (2). The hydrated starting materials $LnCl_3(H_2O)_n$ are readily obtained from the oxides with aqueous hydrochloric acid. After evaporation to dryness at a relatively low temperature in order to avoid partial hydrolysis of the metal chloride to the corresponding oxychloride, water is completely removed by treatment with $SOCl_2$ in DME. Also the cerium and praseodymium derivatives have been prepared according to Eq. (2), with complete consumption of coordinated water.

$$\begin{aligned}&\mathrm{LnCl_3(H_2O)}_n + n\mathrm{SOCl_2} + m\mathrm{DME}\\ &\quad\rightarrow \mathrm{LnCl_3(DME)}_m + n\mathrm{SO_2} + 2n\mathrm{HCl}.\end{aligned} \tag{2}$$

It is interesting to note that the DME adducts of the lanthanide chlorides can also be prepared starting from the appropriate metal carbonate by treatment with $SOCl_2/H_2O/DME$, as exemplified by the erbium and neodymium derivatives. Since neodymium and erbium are separated by eight atomic numbers along the lanthanide series, it is anticipated that this route to the anhydrous DME-solvated chlorides might be successful at least with the other carbonates in between.

For preparative purposes, the metal complexes $[LnCl_3(DME)_2]_n$, $n = 1$ or 2, have been separated by filtration and dried in vacuo at room temperature. However, it should be noted that the derivatives of the early lanthanide elements, namely those in the sequence from lanthanum to neodymium tend to lose DME in vacuo at room temperature giving compounds of analytical composition $LnCl_3(DME)$, presumably polynuclear.

All these compounds show almost superimposable IR spectra with typical bands at 1030–1036, 1076–1079 and 1091–1096 cm^{-1}, attributable to coordinated DME. Extensive use of X-ray diffractometry has been necessary to rationalize the molecular complexity of the products. It has therefore now been established that dinuclear compounds are formed preferentially in the first part of the lanthanide series (from lanthanum to neodymium), whereas mononuclear compounds are systematically present in the second part (from samarium to lutetium), as it will be outlined below. Neodymium appears to be the turning point between the two types of compounds, since it has been isolated both as the dinuclear species, vide infra, and as the mononuclear derivative [12].

We shall describe the mononuclear complexes first.

4. Mononuclear derivatives

The mononuclear adducts $LnCl_3(DME)_2$ from neodymium to lutetium, see Table 1, crystallize in prismatic shapes with the typical habit of Fig. 1. These isotypical compounds have the molecular structure shown in Fig. 2.

The metal is heptacoordinated with a distorted pentagonal bipyramidal geometry where the Cl(1) and Cl(3) atoms occupy the axial positions. The choride ligands form a plane approximately containing the metal and separating the two ethereal ligands on opposite sides.

Within each lanthanide compound the three Ln–Cl distances show little variation, and in some cases are practically identical, see Table 3.

On the contrary, the four Ln–O distances within each lanthanide derivative are significantly different and one short distance [Ln–O(3)], two intermediate distances [Ln–O(1) and Ln–O(2)] and a long one [Ln–O(4)] are present, see Table 4.

The isotypical series is large enough to show a significant trend of metal–ligand distances vs. the number

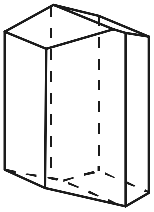

Fig. 1. Crystal habit of the mononuclear complexes $LnCl_3(DME)_2$.

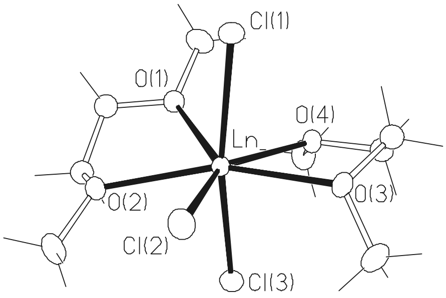

Fig. 2. The molecular structure of the mononuclear lanthanide derivatives $LnCl_3(DME)_2$. Thermal ellipsoids are at 30% probability.

Table 3
Ln–Cl distances (Å) in isotypical $LnCl_3(DME)_2$ structures

Element	Ln–Cl(1)	Ln–Cl(2)	Ln–Cl(3)	Ln–Cl mean
Nd [12]	2.681(1)	2.673(1)	2.682(1)	2.679(1)
Sm [15b]	2.656(1)	2.647(1)	2.656(1)	2.653(1)
Eu	2.643(1)	2.639(1)	2.643(1)	2.639(1)
Gd [10]	2.629(2)	2.625(2)	2.632(2)	2.629(1)
Tb	2.615(1)	2.610(1)	2.617(1)	2.614(1)
Dy [9a]	2.596(1)	2.598(1)	2.599(1)	2.598(1)
Ho	2.592(2)	2.593(2)	2.590(2)	2.591(1)
Er [7b,9b]	2.585(2)	2.582(2)	2.580(2)	2.586(1)
Tm	2.577(3)	2.569(3)	2.573(3)	2.573(2)
Yb	2.558(1)	2.563(1)	2.558(1)	2.559(1)
Lu	2.557(3)	2.551(3)	2.548(3)	2.552(2)

Table 4
Ln–O distances (Å) in isotypical mononuclear $LnCl_3(DME)_2$ complexes[a]

Element	Ln–O(1)	Ln–O(2)	Ln–O(3)	Ln–O(4)
Nd [12]	2.523(2)	2.525(2)	2.481(2)	2.560(2)
Sm [15b]	2.504(3)	2.501(3)	2.448(3)	2.534(3)
Eu	2.481(3)	2.487(3)	2.438(3)	2.513(3)
Gd [10]	2.463(4)	2.474(4)	2.413(4)	2.494(4)
Tb	2.457(4)	2.464(4)	2.405(4)	2.500(4)
Dy [9a]	2.441(3)	2.450(3)	2.396(3)	2.472(3)
Ho	2.436(4)	2.441(5)	2.389(5)	2.478(4)
Er [7b,9b]	2.427(4)	2.423(4)	2.370(4)	2.462(4)
Tm	2.420(7)	2.414(6)	2.368(7)	2.456(7)
Yb	2.413(2)	2.413(2)	2.357(2)	2.449(2)
Lu	2.392(7)	2.390(9)	2.349(8)	2.421(8)

[a] For atom numbering see Fig. 2.

of *f* electrons of the metal ion, and this can be done for the four types of Ln–O distances and for the Ln–Cl distances in the sequence from neodymium to lutetium. [3] As there are no significant differences in the Ln–Cl distances within each lanthanide, see Table 3, the mean values with the appropriate standard deviations have been considered. The plots of Ln–Cl and Ln–O distances vs. the number of *f* electrons of Ln^{3+} are shown in Fig. 3.

A quadratic fit of the plotted values with the function [23] $d(\text{Ln–Cl}) = A_0 - A_1 n + A_2 n^2$, gave the values listed in Table 5 for the A_0, A_1 and A_2 coefficients.

As it can be seen from the values of the coefficients used in the fitting of Ln–Cl and Ln–O(3) distances, A_2 is significantly different from zero.

It is finally worth mentioning that in these isotypical structures the unit cell volume is related to the nature of the central lanthanide. Fig. 4 shows a plot of these data. The cell volumes which have been measured at room temperature well fit the function $U = 1614(3) - 7.7(9)f$

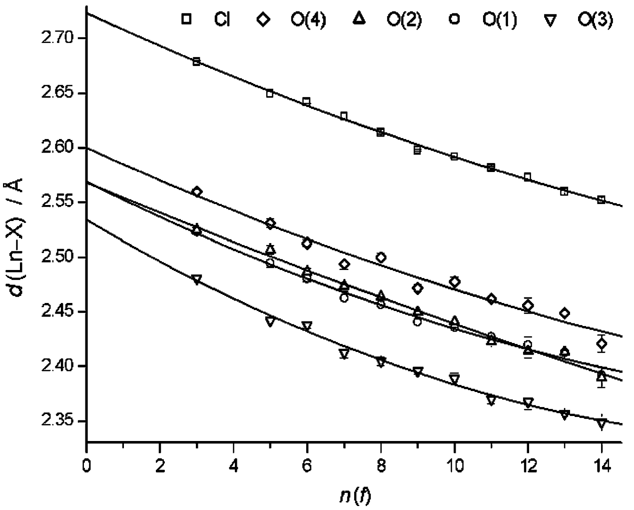

Fig. 3. Fitting of Ln–Cl and Ln–O distances for the mononuclear $LnCl_3(DME)_2$ complexes vs. the number of *f* electrons.

Table 5
Contraction of Ln–X distances: the *A* parameters resulting from the fitting of Fig. 3, and the correlation factor R^2

Bond	A_0	A_1	A_2	R^2
Ln–Cl	2.724(5)	0.016(1)	0.00023(7)	0.997
Ln–O(1)	2.569(9)	0.017(2)	0.0003(1)	0.989
Ln–O(2)	2.568(9)	0.014(2)	0.0001(1)	0.991
Ln–O(3)	2.534(9)	0.020(2)	0.0005(1)	0.991
Ln–O(4)	2.600(17)	0.015(4)	0.0002(2)	0.965

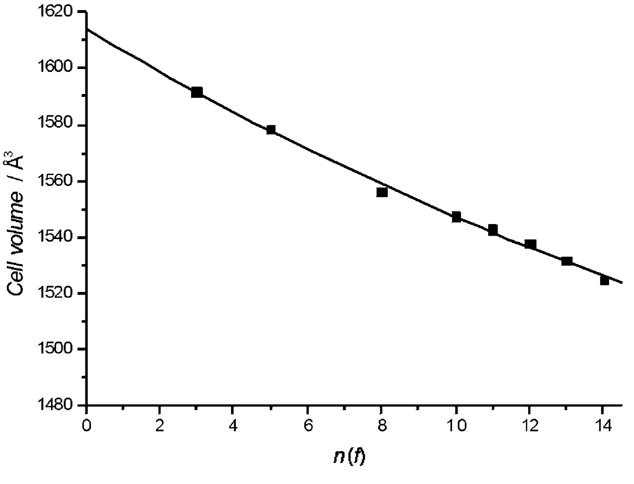

Fig. 4. Fitting of cell volumes of $LnCl_3(DME)_2$ measured at room temperature vs. the number of *f* electrons of the lanthanide. The values referring to the Eu, see Table 1, and Dy [9a] compounds have been omitted from the fitting because data collection for these compounds was carried out at 208 and 203 K, respectively. As far as the Gd derivative is concerned, although the CCDC indicates data collection at room temperature, the considerably lower value of the cell volume [1530 Å^3] reported for this compound suggests that the experiment was actually carried out at a lower temperature.

---

[3] The means and the standard deviations from the means have been calculated [22] by the expressions: $\bar{x} = \sum(x_i/\sigma_i^2)/\sum(1/\sigma_i^2)$; $\sigma(\bar{x} = [1/\sum(1/\sigma_i^2)]^{1/2}$.

$+0.11(5)f^2$, with a correlation factor $R^2 = 0.996$. The cell volumes of the Eu and Dy complexes have been omitted from the fitting because they have been measured at low temperature.

5. Dinuclear derivatives

As the metal radius increases, heptacoordination becomes progressively insufficient to envelop completely the metal centre: with neodymium, octacoordination appears, as shown by a recent X-ray diffractometric experiment on $Nd_2Cl_6(DME)_4$ [9c]. As the atomic number of the lanthanide decreases, the mononuclear species $LnCl_3(DME)_2$, become progressively unstable. The neodymium complex may be considered as the borderline case, for which both the mononuclear [12] and the dinuclear, chloride-bridged dinuclear species $Nd_2Cl_4(\mu_2\text{-}Cl)_2(DME)_4$ [9c] have been identified in the solid state.

As shown by the results of this paper, only dinuclear complexes were observed for lanthanum, cerium and praseodymium. At odds over the mononuclear ones, for which only one crystal phase has been obtained until now, the dinuclear species show an extended polymorphism.

A monoclinic phase with the $P2_1/n$ space group and with the cell parameters listed in the first four columns of Table 2 has been obtained for the La, Ce, Pr and Nd complexes (the products were recrystallized from DME in the temperature gradient from room temperature to about 0 °C). Although the structure of $Nd_2Cl_4(\mu_2\text{-}Cl)_2(DME)_4$ [9c] had already been reported, we decided to investigate the structure of the neodymium derivative, as obtained under our conditions. It constitutes a new phase of $Nd_2Cl_4(\mu_2\text{-}Cl)_2(DME)_4$, that we propose to call α, whose crystals have the habit shown in Fig. 5. They are isotypical with those of $La_2Br_4(\mu_2\text{-}Br)_2(DME)_4$ [7b]. The molecular structure of the α-phase is shown in Fig. 6.

The molecule is centrosymmetric and the coordination polyhedron may be considered as intermediate between the eight-vertex dodecahedron and the bicapped trigonal bipyramid. The four chlorine atoms are arranged around the metal in a sort of flattened tetrahedron, the dinuclear molecule resulting from the sharing of the Cl(1)–Cl(1′) edge. The DME oxygens around the metal centre form another flattened tetrahedron.

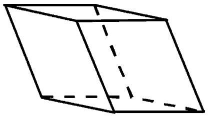

Fig. 5. Crystal habit of $Nd_2Cl_6(DME)_4$.

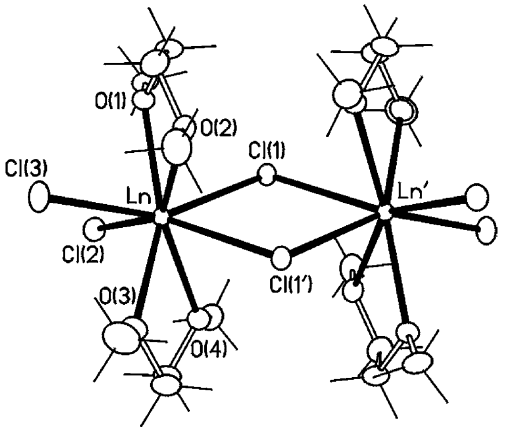

Fig. 6. The molecular structure of α-$Ln_2Cl_6(DME)_4$, Ln = La, Ce, Pr and Nd. Thermal ellipsoids are at 30% probability.

Tables 6 and 7 list the Ln–Cl and Ln–O bond distances for the α-phase of the La, Ce, Pr and Nd dinuclear compounds. For the specific case of neodymium, an interesting comparison can be made about bond distances. The average Nd–Cl bond distance for the *terminal* chloride ligands in our dimer is 2.71 Å, to be compared, see Table 3, with the 2.68 Å average distance of the Nd–Cl bond in the mononuclear compound. Moreover, by comparing the data of Table 4 with those of Table 7, it can be concluded that the Nd–O bond distances in the neodymium dimer are all systematically less than 0.1 Å longer than in the corresponding mononuclear compound.

The Ln–O bond distances of the dinuclear compounds show significantly different values: two are intermediate, one short and one long.

As expected for the increase of the coordination number, the dinuclear complexes are more densely packed than the mononuclear ones. If we compare, in fact, the volume occupied by one unit of $NdCl_3(DME)_2$

Table 6
Ln–Cl distances (Å) in isotypical α-$Ln_2Cl_6(DME)_4$

Element	Ln–Cl(1)	Ln–Cl(1′)	Ln–Cl(2)	Ln–Cl(3)
La	2.902(2)	2.949(2)	2.745(3)	2.791(2)
Ce	2.884(1)	2.927(1)	2.728(1)	2.770(1)
Pr	2.863(1)	2.912(1)	2.709(1)	2.751(1)
Nd	2.849(2)	2.900(1)	2.693(2)	2.742(2)

Table 7
Ln–O distances (Å) in isotypical α-$Ln_2Cl_6(DME)_4$ structures

Element	Ln–O(1)	Ln–O(2)	Ln–O(3)	Ln–O(4)
La	2.623(6)	2.619(6)	2.592(6)	2.674(7)
Ce	2.608(3)	2.600(3)	2.584(3)	2.666(4)
Pr	2.587(2)	2.586(3)	2.574(2)	2.654(3)
Nd	2.575(4)	2.573(4)	2.556(4)	2.637(4)

in the mononuclear case ($V/Z = 397.9$ Å^3) with the volume occupied by the same unit in the dinuclear compound [$V'/(2 \cdot Z') = 383.5$ Å^3], we observe a decrease of 3.6%.

By recrystallizing the α-phase of $Pr_2Cl_6(DME)_4$ from DME, we found prismatic crystals with a more elongated shape, in addition to the crystals with the habit of Fig. 5. One of them showed the same monoclinic space group $P2_1/n$ as the α-phase, but a different unit cell ($a = 8.474$, $b = 18.149$, $c = 10.569$ Å; $\beta = 109.16°$), see Table 2. Its crystal structure solution showed to be a polymorph of the α-phase, built by molecules with the same conformation, but with a different packing. Fig. 7 shows a comparison between the crystal structures of the α-phase and the new one that we propose to call β.

The more evident difference between the two structures can be found in the disposition of the $\{Pr_2Cl_2\}$ lozenges forming the central units of the molecules. In the structure of the α-phase they are lying on parallel planes, while in the β one the lozenges of adjacent rows are disposed on almost perpendicular planes. This corresponds to a slightly more efficient packing and, consequently, to a higher density.

At the present time, only the α-phase of the dinuclear complexes of lanthanum(III), and cerium(III) have been found. In our recrystallizations of the neodymium derivatives, we have identified crystals of another type, shaped as little sticks. These crystals correspond to a new solvated phase of $Nd_2Cl_6(DME)_4 \cdot DME$. They belong to the triclinic space group $P\bar{1}$, with cell parameters: $a = 8.645$, $b = 9.322$, $c = 12.676$ Å; $\alpha = 88.60$, $\beta = 83.88$, $\gamma = 65.78°$. The molecular structure of the dinuclear compound is shown in Fig. 8.

Also this dinuclear complex is centrosymmetric, but performs a different conformation with respect to that of the α-phase. As it can be seen, the Cl(1) Cl(1′) Cl(2) and Cl(3) atoms around neodymium form a distorted trigonal pyramid, with the metal lying on the basal plane. The coordination geometry around the metal is approximately square antiprismatic. It is almost, but not exactly, superimposable to the conformation observed in the recently described structure of unsolvated $Nd_2Cl_6(DME)_4$ [9c], that we propose to identify as the γ-phase.

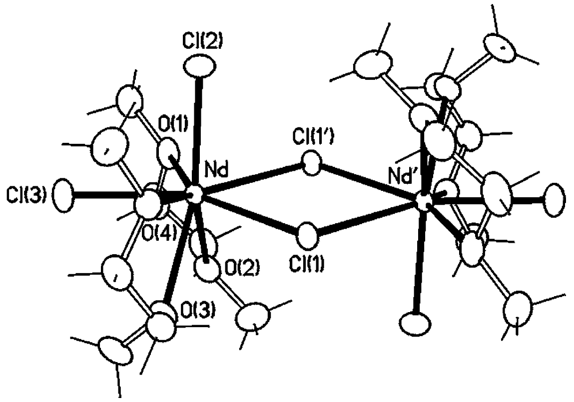

Fig. 8. The molecular structure of $Nd_2Cl_6(DME)_4 \cdot DME$. Thermal ellipsoids are at 30% probability.

The Ln–Cl and Ln–O distances of $Nd_2Cl_6(DME)_4 \cdot DME$ are listed in Table 8. The interatomic distances are very similar to those of the γ-phase. No bonding interactions with the uncoordinated DME molecules are present in this neodymium complex. As displayed in Fig. 9, the additional DME molecules forming the crystal constitute a spacer layer between adjacent dinuclear molecules.

Table 8
Bond distances (Å) in $Nd_2Cl_6(DME)_4 \cdot DME$

Ln–Cl(1)	2.828(1)	Ln–O(1)	2.592(4)
Ln–Cl(1′)	2.958(1)	Ln–O(2)	2.503(4)
Ln–Cl(2)	2.661(1)	Ln–O(3)	2.604(4)
Ln–Cl(3)	2.708(1)	Ln–O(4)	2.631(4)

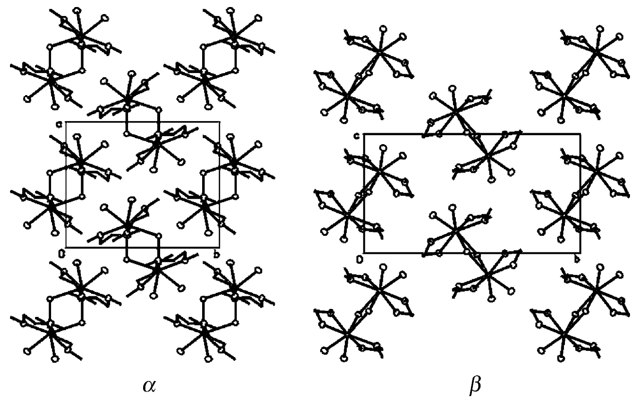

Fig. 7. The different crystal structures of α and β-$Pr_2Cl_6(DME)_4$. The molecules are projected down **c** and down **a**, respectively.

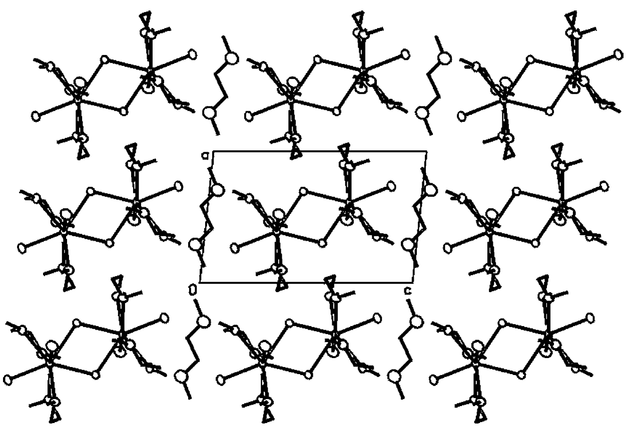

Fig. 9. Crystal structure of $Nd_2Cl_6(DME)_4 \cdot DME$ projected down **b**.

6. Conclusions

Three different methods for the preparation of the DME adducts of lanthanide trichlorides are presented in this paper, starting from the readily available oxide, from the hydrated chlorides or from the carbonates, thus substantially covering the whole series of lanthanide elements. The methods operate at room temperature, and as long as moisture is avoided, no special care should be taken to operate under an inert atmosphere. The failure of the oxides of terbium and ytterbium, i.e. towards the end of the series, to undergo chlorination by the $SOCl_2$/DME/H_2O system is believed to be thermodynamic in nature and related to the elevated lattice energy of the oxide.

The new structural information from this paper shows that the lighter lanthanides, characterized by a relatively large ionic radius, form isotypical dinuclear $Ln_2Cl_6(DME)_4$ complexes. Although cases of polymorphism have been identified, in all cases the central metal atom is octacoordinated in the dinuclear species. For neodymium, in addition to the already known [12] mononuclear species $NdCl_3(DME)_2$, also the dinuclear $Nd_2Cl_6(DME)_4$ has been identified in the framework of the present study. Thus, neodymium, with its relatively large ionic radius, appears to be the borderline element for which heptacoordination in the mononuclear $NdCl_3(DME)_2$ derivative and octacoordination in $Nd_2Cl_6(DME)_4$ are characterized by a small energy difference and substantially even coexist in the solid state.

The observation that the DME adducts of the early lanthanide chlorides tend to lose DME at room temperature giving presumably polynuclear chloride-bridged products of analytical composition $LnCl_3$ (DME) can be related to the structural properties of the trichlorides themselves [24]. Along the lanthanide series, enneacoordination, typical of UCl_3, is found for the elements from lanthanum to gadolinium; terbium is unique in performing CN = 8, while the subsequent elements from dysprosium to lutetium are hexacoordinated. Clearly the stabilization induced by DME smooths out the differences within the second part of the series, thus giving a homogeneous set of isostructural species.

It is easily predicted that the DME adducts of lanthanide chlorides, which are easily prepared as shown in this paper, will experience an extended utilization in synthetic lanthanide chemistry in non-aqueous media, due to their low nuclearity and to their solubility in organic solvents. Already some uses of these precursors can be found in the recent literature, as applied to both Main Group and lanthanide elements [25].

7. Supporting information available

Crystallographic data (excluding structure factors) for all compounds have been deposited with the Cambridge Crystallographic Data Centre with the reference numbers which follow. For the $LnCl_3(DME)_2$ series (Ln = Eu, Tb, Ho, Tm, Yb, Lu): CCDC 211399, CCDC 211400, CCDC 211401, CCDC 211402, CCDC 211403, CCDC 211404, respectively; for the α-$Ln_2Cl_6(DME)_4$ series (Ln = La, Ce, Pr, Nd): CCDC 211405, CCDC 211406, CCDC 211407, CCDC 211408, respectively; for $Nd_2Cl_6(DME)_4 \cdot DME$: CCDC 211409; and for β-$Pr_2Cl_6(DME)_4$: CCDC 211410. Copies of the data can be obtained, free of charge, on application to CCDC, 12 Union Road, Cambridge CB2 1EZ, UK, (fax: +44 1223 336033 or deposit@ccdc.cam.ac.uk).

Acknowledgements

The authors wish to thank the Ministero dell' Istruzione, dell' Universitàe della Ricerca (MIUR), Programmi di Ricerca Scientifica di Rilevante Interesse Nazionale, Cofinanziamento 2002–2003, the Consiglio Nazionale delle Ricerche (CNR), Materiali Speciali per Tecnologie Avanzate II (MSTA II), Roma, for financial support of this work, and Rhône-Poulenc for a generous gift of lanthanide oxides. Thanks are due to Dr. Alessandra Merigo for some preliminary synthetic experiments.

References

[1] F. Priolo, G. Franzo, S. Coffa, A. Carnera, Mater. Chem. Phys. 54 (1998) 273.

[2] (a) L. Porri, A. Giarrusso, in: G.C. Eastmond, A. Ledwith, S. Russo, P. Sigwalt (Eds.), Comprehensive Polymer Science Part II, vol. 4, Pergamon Press, Oxford, UK, 1989, p. 53;
(b) A. Fischbach, F. Perdith, W. Scherer, R. Anwander, Organometallics 21 (2002) 4569.

[3] J.A. Cowan, Inorganic Biochemistry, VCH, Weinheim, 1993.

[4] T. Imamoto, Lanthanides in Organic Synthesis, Academic Press, London, 1994.

[5] D. Belli Dell'Amico, F. Calderazzo, C. Della Porta, A. Merigo, P. Biagini, G. Lugli, T. Wagner, Inorg. Chim. Acta 240 (1995) 1.

[6] S. Petricek, A. Demšar, L. Golic, Polyhedron 18 (1999) 529.

[7] (a) G.B. Deacon, T. Feng, P.C. Junk, B.W. Skelton, A.N. Sobolev, A.H. White, Aust. J. Chem. 51 (1998) 75;
(b) G.B. Deacon, T. Feng, P.C. Junk, G. Meyer, N.M. Scott, B.W. Skelton, A.H. White, Aust. J. Chem. 53 (2000) 853.

[8] (a) J.B. Reed, B.S. Hopkins, L.F. Audrieth, Inorg. Syn. 1 (1939) 28;
(b) G.B. Deacon, T.D. Tuong, D.L. Wilkinson, Inorg. Syn. 27 (1990) 136.

[9] (a) S. Anfang, K. Denicke, J. Magull, Z. Naturforsch. 51B (1996) 531;
(b) S. Anfang, M. Karl, N. Faza, W. Massa, J. Magull, K. Denicke, Z. Anorg. Allgem. Chem. 623 (1997) 1425;
(c) G.B. Deacon, D.J. Evans, P.C. Junk, Z. Anorg. Allgem. Chem. 628 (2002) 2033.

[10] W. Gecheng, G. Hanrong, J. Zhongsheng, S. Qi, Jegou Huaxue, J. Struct. Chem. (Chin.) 8 (1989) 61, The X-ray data have been obtained through the CCDC.

[11] W.J. Evans, T.J. Boyle, J.W. Ziller, J. Am. Chem. Soc. 115 (1993) 5084.

[12] G. Zi, H.-W. Li, Z. Xie, Organometallics 21 (2002) 1136.

[13] U. Abram, D. Belli Dell'Amico, F. Calderazzo, C. Della Porta, U. Englert, F. Marchetti, A. Merigo, Chem. Commun. (1999) 2053.

[14] D.H. Templeton, C.H. Dauben, J. Am. Chem. Soc. 76 (1954) 5237.

[15] (a) N.N. Greenwood, A. Earnshaw, Chemistry of the Elements, Pergamon Press, Oxford, 1989, p. 1437;
(b) U. Baisch, W. Schnick, Z. Anorg. Allg. Chem., in press.

[16] XSCANS, X-ray Single Crystal Analysis System, rel. 2.1 Siemens Analytical X-ray Instruments Inc., Madison, Wisconsin, USA, 1994.

[17] G.M. Sheldrick, Programs for Crystal Structure Analysis (Release 97-2), Institut für Anorganische Chemie der Universität, Tammanstrasse 4, D-3400 Göttingen, Germany, 1998.

[18] G.M. Sheldrick, SHELXTL-Plus, Rel. 5.1, Siemens Analytical X-Ray Instruments Inc., Madison, Wisconsin, USA, 1997.

[19] M.D. Taylor, Chem. Rev. 62 (1962) 503.

[20] (a) V. Gutmann, J. Phys. Chem. 63 (1959) 378;
(b) M. Baaz, V. Gutmann, L. Hübner, J. Inorg. Nucl. Chem. 18 (1961) 276.

[21] P.B. Arimondo, F. Calderazzo, R. Hiemeyer, C. Maichle-Mössmer, F. Marchetti, G. Pampaloni, J. Strähle, Inorg. Chem. 37 (1998) 5507.

[22] W.C. Hamilton, Statistics in Physical Science, The Ronald Press Company, New York, 1964, p. 43.

[23] (a) E.A. Quadrelli, Inorg. Chem. 41 (2002) 167;
(b) B. Deng, D.E. Ellis, J.A. Ibers, Inorg. Chem. 41 (2002) 5716.

[24] A.F. Wells, Structural Inorganic Chemistry, fifth ed., Clarendon Press, Oxford, 1984.

[25] (a) B. Bogdanovic, N. Janke, H.-G. Kinzelmann, U. Westeppe, Chem. Ber. 121 (1988) 33;
(b) G. Stieglitz, B. Neumüller, K. Dehnicke, Z. Naturforsch. 48b (1993) 730;
(c) P. Lohner, J. Fischer, M. Pfeffer, Inorg. Chim. Acta 330 (2002) 220;
(d) C. Jones, P.C. Junk, J.W. Steed, R.C. Thomas, T.C. Williams, J. Chem. Soc., Dalton Trans. (2001) 3219;
(e) I. Korobkov, G. Aharonian, S. Gambarotta, G.P.A. Yap, Organometallics 21 (2002) 4899.